The Pennsylvania State University

The Graduate School

College of Engineering

WIRELESS POWER TRANSFER FOR WIRELESS SENSOR MODULES

A Thesis in

Electrical Engineering

by

Submitted in Partial Fulfillment
of the Requirements
for the Degree of

Master of Science

December 2009

The thesis of Aseem Singh was reviewed and approved* by the following:

Sven G. Bilén
Associate Professor of Engineering Design, Electrical Engineering, and Aerospace Engineering
Thesis Advisor

James Breakall
Professor of Electrical Engineering

Kenneth Jenkins
Professor of Electrical Engineering
Department Head of Electrical Engineering

*Signatures are on file in the Graduate School

ABSTRACT

Engineering solutions to the development of techniques to transfer power without any physical medium have been envisioned for quite some time to mitigate the complexity involved in the wiring of electronic and electrical systems. Various attempts to demonstrate power-beaming phenomena have met with some success, as industry keeps searching for new approaches and methods. Our work has been involved with the specific application of a wireless power transmission system to be used on the heat shield of a spacecraft. A proof-of-concept design to power multiple sensor modules energized by a central transmitter station has been designed and tested. During the course of the project, interesting observations have been noted and documented. With limited available research on the topic, we have proposed and formulated theoretical analyses and conclusions based on observational data derived from the tests performed on the modules built. This work contributes to this new, little explored area of research, and suggests future uses of the system for other applications.

ACKNOWLEDGMENTS

I would like to acknowledge and thank all the people associated with this project and who have helped me throughout my education here at Penn State. I am grateful to my adviser, Dr. Sven Bilén, for giving me this incredible opportunity to be a part of his research group, and work with him on this project. He has been a tremendous support and I also appreciate the belief he showed in me throughout my duration here.

I would also like to acknowledge the help I got from my other research members, and faculty in the department whenever I had questions that I could not answer by myself. A special mention about my family and friends who have supported my decisions, and have helped me finish my studies at Penn State.

I would like to acknowledge the generous support of NASA's Constellation University Institutes Project (CUIP) for my graduate research assistantship.

Finally, I would like to acknowledge my university, Penn State that provided the resources and an environment conducive for world-class research, and also has the ethics and culture for a great social and emotional growth besides academic progress.

TABLE OF CONTENTS

LIST OF TABLES

LIST OF FIGURES

Chapter 1

Introduction

Spacecraft and Payload Systems (SPS) typically contain complex Wiring and Interconnection Subsystems (WICS). These subsystems are sources of multiple failure mechanisms including, but not limited to, shorts, opens, chafing, sparking, ageing, and connector interface issues. WICS also add volume, weight, and complexity to the SPS design. It has been suggested that eliminating the long wires, cables, and connector interfaces typical throughout these interconnection subsystems could potentially revolutionize spacecraft and payload design. An SPS, without the constraints imposed by complex wiring subsystems, can be configured for optimized physical partitioning and placement of SPS components and hardware Configuration Items (CI). Furthermore, SPS reliability and survivability improvements can be expected because of the elimination of the multiple failure modes inherent to current WICS.

Introduction of Wireless Sensor Subsystem (WLSS) technology into SPS Thermal Protection Systems (TPS) has been proposed as proof-of-concept project. The objective of the project is to design, develop, test and verify the functionality and performance of a WLSS that has been integrated into a SPS TPS. The WLSS concept for the TPS includes the signal conditioning, conversion, processing, command, control, and data transfer elements capable of transmitting the sensor data to a centralized WLSS data receiving element. The WLSS for TPS concept also eliminates the use of battery-based power supplies through the introduction power beaming technology to provide power to the WLSS modules.

This thesis will present the research and theoretical foundation for implementation of a Wireless Power Transfer technique used to develop a viable Wireless Power Beaming Subsystem (WPBS) for use in WLSS applications.

1-1 Contributions of this Work and Other Applications

This work explores a challenging and eccentric area of research. The idea of sending power without using a physical medium was first envisioned more than a century ago [*Brown,* 1984]. Since then, measurable progress has been made towards understanding the functionality of such an abstruse phenomenon, which although having existed in the research phase for many years, has not been satisfactorily conceptualized or theoretically proven to date. This thesis provides insight into the working of a vastly unexplored region of engineering and physics and we believe we have obtained results that will open new vistas for future research.

The successful demonstration of a wireless power transfer system would be enabling for numerous other applications. Some of the methods employed in consumer electronics relating to charging of notebooks, cell phones, or toothbrushes still requires near physical contact with the charging pad. However, with the advancement, development, and utilization of wireless power transfer systems, the path to expansion for use in larger and more complex systems is visible and achievable. Application and adaptation to satellites and spacecraft for power control and distribution during flight, or industrial applications such as charging and powering robots and computers, or commercial applications for operation of low power appliances without physical wiring is discussed. Some details regarding improvements of the system and future work will describe the techniques that might be employed to increase the efficiency and the overall range of the system.

1-2 Overview of the Thesis

This thesis describes a proof-of-concept WLSS system as a viable solution for the internal wiring issues experienced on spacecraft, and more specifically the focus on wireless power delivery to these modules. The thesis also projects future applicability and widespread use

of the system throughout the aerospace and defense industry including government and commercial applications.

The problem description in Chapter 1 outlines the need for alternate concepts and solutions for the issues that continue to plague WICS. The author wishes to note that, although most of the research conducted and conceptual solutions developed may be tailored to specific customer-defined requirements, the research and solutions have applicability to a wide range of applications, industries, and products.

The background and literature review in Chapter 2 discusses efforts, concepts, and systems previously developed as potential solutions. A discussion of the baseline concept that was utilized and exploited to develop the system and the theoretical analysis of the phenomena enabling functionality of the system is described. The applicable mathematical equations are delineated herein. Note that the papers containing the mathematical proofs are contained in References section.

Next, the baseline objectives, allocated requirements, specifications, and components of the system are presented in Chapter 3 along with a description of the design, development, assembly, test, and evaluation of the system. The selected components are described in detail as are the rational and justification for each choice.

The characterization, test, and evaluation of the system is introduced in Chapter 4 and discussed and the test purpose, objectives, and procedures are presented. The test data, observations, and subsequent analyses enabled formulation of enhanced theoretical concepts. Lastly, in Chapter 5 the summary and future scope of the research is discussed. Although the system is currently in an early proof-of-concept stage, the improvements over legacy systems are very evident and tangible. An approach and suggestions for continuation of the system characterization, verification, and validation are also presented.

Chapter 2

Background and Literature Review

This chapter describes the previous attempts made at accomplishing power beaming, followed by the mathematical analysis and theory behind the technology that was implemented. An initial description of our system built here and then some current systems exploring the wireless power transfer are stated in the later part of the chapter. Following is the summation of all the theories that were investigated and reviewed.

2-1 Inductive Coupling

The transformer action is one of the simplest examples of wireless power transfer. The primary and secondary sides are separated from each other by an air gap. The energy transfer takes place by the process of mutual induction. The main problem with this method is the large primary and secondary leakage inductances. Therefore, primary and secondary compensation of the leakage inductances is required, i.e., the series resonance capacitance on the primary side and parallel secondary capacitance on the secondary side.

For high frequencies, smaller filter elements and ferrite components can be used and the transmitted electric power and the efficiency can be increased considerably by utilizing a special inverter, the Phase-Shift Controlled IGBT (Insulated Gate Bipolar Transistor) Bridge at the primary side. Using an experimental arrangement [*Mecke and Rathge,* 2004] with a controlled constant level of 560 V, 1 kW of electric power has been transferred through an air gap of 300 mm at 100-kHz transmission frequency, at an efficiency of 80%.

2-2 Resonant Induction

Electromagnetic waves in a highly angular waveguide produce evanescent waves that carry no energy. If a proper resonant waveguide is brought near the transmitter, the evanescent waves can allow the energy to tunnel to the power drawing waveguide, where they can be rectified into DC power. Since the electromagnetic waves tunnel, they would not propagate through the air to be absorbed or dissipated, and would not disrupt electronic devices or cause physical injury. The range of this method is anticipated to be up to 5 meters [*Brown*, 1984].

Aristeidis Karalis and other researchers at the Massachusetts Institute of Technology applied this near field behavior on their functional prototype [*Karalis et al.*, 2008].

2-3 Microwave Power Transfer

Heinrich Rudolf Hertz performed one of the first experiments in the area of wireless transmission using radio waves in 1888. Guglielmo Marconi and Nikola Tesla worked further in this area and investigated radio transmission and reception. Power transmission via radio waves can be made more directional, allowing power beaming over longer distances, with shorter wavelengths of electromagnetic radiation, typically in the microwave range. A rectenna may be used to convert the microwave energy back into electricity. Rectenna [*Mickle et al.,* 2001] conversion efficiencies exceeding 95% have been realized. Power beaming using microwaves [*Minhong et al.*, 2005] has been proposed for the transmission of energy from orbiting solar power satellites to Earth and the beaming of power to spacecraft leaving orbit has been considered.

2-4 Laser Power Transfer

Power can also be transmitted by converting electricity into a laser beam that is targeted at a solar cell receiver. Generally known as “power beaming”, this system is moderately inefficient in the conversion of electricity to light and conversion of light to electricity. Additionally, these systems require a direct line of light from source to target.

2-5 Electrical Conduction

In electrical conduction electrical currents are made to flow through naturally existing conductors, such as the earth, lakes, oceans, and the atmosphere. These natural media become conductive when the breakdown voltage is exceeded and the gas becomes ionized. In a practical wireless energy transfer system using this principle, a high power ultraviolet beam might be used to form a vertical ionized channel in the air directly above the transmitter-receiver stations.

Table 1 below summarizes all the techniques of wireless power transfer investigated and relevant characteristics for each method.

Table 1 Review/Selection of Technology

	Induction	**Resonance**	**Rectenna/ Microwave**	**Light**	**Conduction**
Principle/Theory	Electromagnetic induction	Resonance coupling	Photovoltaic-effect	Photovoltaic effect	Electric/ Magnetic Fields
Development Stage	Commercial	Research	Commercial	Commercial	Theory
Peak Energy Com.	Pending primary source	—	85%	10–15%, sust. 120 W	—
Peak Energy Lab	Sustaining 4000 W	40%	95%	50%	—
Energy Source	Electric grid	Electric grid	Electric grid/Solar	Solar source	Electric grid
Cost	Inexpensive	Moderate	Expensive	Moderate	Expensive
Operating Freq.	<1500 Hz	10e6 Hz	3e9–3e12 Hz	4e14–8e14 Hz	—
Line of Sight	No	No	Yes	Yes	No
Effective Distance	Short	Mid	Long	Long	Long
Company/Org	P&G, Splash Power	MIT, Marin Soljacic	Raytheon	BP, SANYO	—

2-6 Non-Radiative Mid-Range Strongly Coupled Magnetic Resonance Power Transfer

In the early 20th century, before the electrical power grid, Nikola Tesla devoted much effort to develop techniques to transport energy without any carrier medium. The efforts [*Salter et al.*, 2007; *Bansal,* 2004; *Popovic,* 2006; *Browdowsky*, 1996] were met with limited success, as the experiments involved undesirably large electric fields. The efficiency of power transfer is very low if the radiation is omnidirectional; and unidirectional radiation requires an uninterrupted line of sight and sophisticated mechanisms. A recent paper [*Kurs et al.,* 2007] and experiment at MIT and Intel presented an analysis of the feasibility of using resonant objects coupled through their nonradiative fields for mid range energy transfer.

Two resonant objects of the same resonant frequency tend to exchange energy efficiently, while dissipating relatively little energy in off-resonant objects. If one can operate in the "strongly coupled" regime of operation, the energy transfer is expected to be very efficient. In this work, we focus on one particular physical embodiment: magnetic resonance. We were able to identify the strongly coupled regime in the system of two coupled magnetic resonances by exploring near field magnetic resonant induction at megahertz frequencies. At first, it may seem like typical magnetic induction. Efficient power transfer occurs in particular regions of the parameter space describing resonant objects strongly coupled to one another. Using coupled-mode theory to describe the system, we obtain the following equation:

$$\dot{a}_m(t) = (j\omega_m - \Gamma_m)a_m(t) + \sum_{n \neq m} j\kappa_{mn}a_n(t) + F_m(t)\,, \tag{1}$$

where the indices denote the different resonant objects. The variables $a_m(t)$ are defined so that the energy in the object m is $|a_m(t)|^2$, ω_m is the resonant angular frequency of that object, and Γ_m is its intrinsic decay rate due to absorption, radiated losses, etc. In this framework, an uncoupled and undriven oscillator with parameters ω_0 and Γ_0 would evolve in time as $\exp(j\omega_0 t - \Gamma_0 t)$. The

$\kappa_{mn} = \kappa_{nm}$ are coupling coefficients between the resonant objects indicated by the subscripts, and $F_m(t)$ are driving terms.

Our power beaming system can be analyzed at a more basic level of two components *viz.* a transmitter and a receiver (denoted by subscripts *T* and *R*). The two objects have a coupling coefficient, κ, and the work is extracted by means of a load (denoted by *W*) that acts as a circuit resistance, and has the effect of contributing an additional term Γ_w to the unloaded receiver object's decay rate Γ_R. The overall decay rate at the receiver side is thus $\Gamma'_R = \Gamma_R + \Gamma_w$. The work extracted is determined by the power dissipated in the load that is, $2\Gamma_w|a_D(t)|^2$. Maximizing the efficiency η is equivalent to solving the impedance matching problem. It can be shown that the system works best when the receiver and transmitter are resonant, in which case the efficiency is given by,

$$\eta = \frac{\Gamma_w |a_R|^2}{\Gamma_T |a_T|^2 + (\Gamma_R + \Gamma_w)|a_R|^2}$$

$$= \frac{\frac{\Gamma_w}{\Gamma_R}\frac{\kappa^2}{\Gamma_T \Gamma_R}}{\left[\left(1+\frac{\Gamma_w}{\Gamma_R}\right)\frac{\kappa^2}{\Gamma_T \Gamma_R}\right] + \left[\left(1+\frac{\Gamma_w}{\Gamma_R}\right)^2\right]} \qquad (2)$$

The efficiency is maximized when $\Gamma_w/\Gamma_R = [1 + (\kappa^2/\Gamma_T\Gamma_R)]^{1/2}$. It is easy to show that the key to efficient energy transfer is to have $\kappa^2/\Gamma_T\Gamma_R > 1$. This is the strong coupling regime of operation that we have exploited for our experiments and system. Resonance plays an essential role in this power transfer mechanism, as the efficiency is improved by approximately ω^2/Γ_R^2 ($\sim 10^6$ for typical parameters) relative to the case of inductively coupled non-resonant objects.

2-7 Theoretical Model for Self-Resonant Antennas

The transmitter and the receiver sides consist basically of antennas that resonate at similar frequencies, the receiver is coupled inductively to a rectifier circuit, and the transmitter is stand-alone, but may be modified with matching circuits in later stages. The system [*Kurs et al.,* 2007] relies on the interplay of distributed inductance and distributed capacitance to achieve resonance. The antennas are selected to be helix coils, of *n* turns, radius *r*, and height *h*. The literature has no solution for a theoretical model of a finite helix describing the distributed inductance and capacitance, and even in the case of infinitely long coils; the solutions rely on assumptions that are inadequate for our system.

The energy contained in the helix is at certain points in time completely due to the current, and at other points it is completely due to the charge. Using electromagnetic theory, we can define an effective inductance *L* and an effective capacitance *C* for each coil as follows:

$$L = \frac{\mu_0}{4\pi |I_0|^2} \iint dr dr' \frac{J(r).J(r')}{|r - r'|}, \tag{3}$$

$$\frac{1}{C} = \frac{1}{4\pi\varepsilon_0 |q_0|^2} \iint dr dr' \frac{\rho(r)\rho(r')}{|r - r'|}. \tag{4}$$

The spatial current **J**(**r**) and charge density **ρ**(**r**) are obtained from the current and charge densities along the coil. As defined, *L* and *C* have the property that the energy contained in the coil is given by

$$U = \frac{1}{2} L |I_0|^2$$

$$= \frac{1}{2C} |q_0|^2. \tag{5}$$

Given this relation and the equation of continuity, the resulting resonant frequency is $f_0 = 1/[2\pi(LC)^{1/2}]$. We can now treat this coil as a standard oscillator in coupled mode theory by defining $a(t) = [(L/2)^{1/2}]I_0(t)$.

The coupled-mode theory decay constant for the coil is therefore $\Gamma = (R_0+R_r)/2L$, and its quality factor is $Q = (\omega/2\Gamma)$. The coupling coefficient can be determined by looking at the power transferred from the source to the device coil, assuming a steady-state solution, and it is given as $\kappa = \omega M/[2(L_T L_R)^{1/2}]$. When the distance D between the centers of the two coils is much larger than their characteristic size, κ scales with D^{-3} dependence characteristic. Both κ and Γ are functions of frequency, and κ/Γ and the efficiency are maximized for a particular value of f.

2-8 Selection of Technology

Heat shield technology is a critical component of manned and unmanned spaceflight. In particular, the new Crew Exploration Vehicle (CEV) requires thermal protection systems (TPS) beyond the current state of the art. Although new TPSs are under development, a key unknown is the performance of current TPSs. To address this unknown, technology-demonstrator missions with the ability to diagnose TPS performance during reentry are currently in the planning stages. This requires an instrumented TPS, which may contain thermocouples, radiometers, spectrometers, pressure sensors, and accelerometers to provide data on the flow, thermal radiation, and ablation rates. However, one major barrier to integrating these sensors is the complexity involved in installing the instrumentation and its associated wiring into a five-meter-class heat shield.

This work is part of a system being developed called "TPS*Link*" to wirelessly power and collect data from sensors that instrument TPSs. The system consists of a "TPS*Link* Manager" that interfaces with the spacecraft and beams power to each of 1-to-*n* "TPS*Link* Nodes", as well as

sets up wireless data links to each of the TPS*Link* Nodes. This wireless sensor system would replace bulky wire harnesses that may have runs of 10+ meters, i.e., from the sensor to heat shield edge and back into a data collection unit. Each of the nodes will be extremely lightweight and very small, placing minimal requirements for secure attachment to the TPS itself. The following is an overview of the system and the elementary structure. Figure 1 shows the schematic of the TPS*Link* concept.

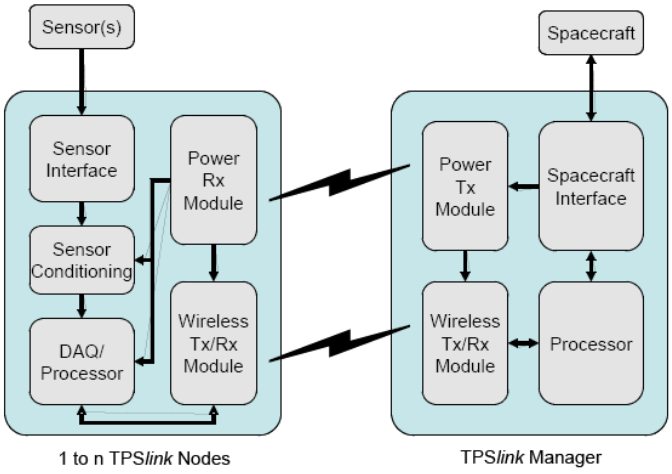

Figure 1 TPS*Link* concept

For this project, the overall system can be broken up into four major parts: the transmitter, the receiver, the sensors, and the communication module. An explanation of the various components of the specifications and the minimum, maximum, or the optimum limit is tabulated.

The technology that was selected uses the RF near field region and having resonant coupling between the transmitter and receiver systems. This system has higher efficiency compared to most other system at higher ranges. One of the prime factors for this selection was the compact structure of the transmitter and receiver modules. The rest of the thesis explains the different aspects of the system that was developed and tested.

2-9 Some Recent Developments

The interest in wireless power transfer recently has increased significantly. Hence, new developments are being reported often and it is instructive to provide some information on these reports.

Sony develops a highly efficient power transfer system based on magnetic resonance.

Sony Corporation developed the wireless power transfer system capable of beaming up to 60 watts of power over a distance of 50 cm with an efficiency of 80% [*www.sony.net,* Oct. 2009]. The main features of the system are high speed rectifier and use of passive extender units to extend the transfer distance.

With the growth in networked products, the number of cables used to connect these products has also increased. While data cables are rapidly being replaced with wireless communication systems, the demand for WPT systems is also growing. Sony looks to proceed with its efforts to develop and work more on further technologies to improve their system.

University of Tokyo, Wireless Power Transfer for Electric Vehicles

In their paper [*Imura et al.,* 2009], the feasibility of wireless power transfer for electric vehicles by electromagnetic resonant coupling is studied. They worked on small sized antennas that can be equipped on the bottom of the vehicle and the electrical characteristics with equivalent circuits.

Chapter 3

Power Beaming Subsystem

High level system requirements were provided by NASA Ames Research Center and developed through technical interchange and coordination with the research team. This chapter provides the details of the power beaming system that led to the development of the hardware and the conversion of theoretical concepts into a proof-of-concept hardware.

3-1 Transmitter

The power transmission/antenna system with the following characteristics was evaluated and characterized (note: "TBD" is provided in these specifications when the value is not yet specified):

- Radiation Pattern. Omnidirectional transmitting antenna.
- Compact in size. Size constraints were driven by the stakeholder's needs.
- Power requirements. The system application allocated a requirement of 1 watt of power transfer
- Frequency of Operation. The frequency of operation must be compatible with and non-interfering with the ZigBee sub-system.
- Bandwidth. The antenna shall have a bandwidth of about 30 MHz.
- Cost. Low recurring cost shall be a requirement for the antenna with a goal of TBD.

3-1-1 Transmitter Specifications

The transmitter antenna shall transmit a sinusoidal signal at selected power levels. The specifications for the transmitter are as follows:

- An input voltage as delineated in Table 2 shall be supplied to the transmitting antenna.
- The input current delineated in Table 2 shall be supplied at the terminal of the transmitter.
- The input power shall be TBD.
- The power and frequency shall be as delineated in Table 2 and shall be selected to obtain optimum power generation at the receiver. It may be noted here that the selection of frequency is dependent on the requirements provided by NASA, with respect to some "keep-out zones" in the frequency band utilized on a spacecraft. We were allotted two frequency bands for our work, 300–350 MHz and 900–925 MHz, to ensure of minimal interference with other components/processes. Hence, our antenna selection is largely based on considering this factor, as may be seen in the further description of the system.

Table 2 Transmitter Specifications

Parameter	Value
V_{max}	<20 V
V_{min}	~10 V
I_{max}	~100 mA
I_{min}	2 mA
P_{max}	2 W
P_{min}	1 W
Frequency	315 MHz

Additional transmitter design constraints are listed in Table 3

Table 3 Transmitter Design Constraints

Parameter	Value
Weight	<1 kg
Dimensions	3″ × 3″ × 3″
Waveform	Sinusoidal
Housing Material	TPS Material
Temperature	TBD
Range	5 m
Cost	TBD

3-1-2 Antenna Selection for Transmitter

Several transmitter omnidirectional antennas were evaluated as described in the following sections.

3-1-2-1 Splatch ANT 315 SP Antenna

Table 4 lists the Splatch ANT 315P antenna electrical characteristics and Figure 2 depicts the physical characteristics:

Table 4 ANT 315 SP Antenna Electrical Characteristics [*Antenna Factor Inc.*]

Parameter	Value
Center Frequency	315 MHz
Bandwidth	5 MHz
Wavelength	Quarter wave
Impedance	50 Ω
Connection	Surface Mount

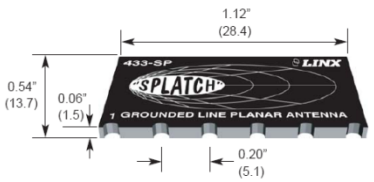

Figure 2 Splatch ANT 315 SP Antenna Physical Characteristics [*Antenna Factor Inc.*]

For initial testing of the concept, the Splatch ANT-315-SP was primary choice due to the omni-directionality of the radiation pattern.

3-1-2-2 ANT-916-JJB-xx

The JJB series [*Antenna Factor Inc.*] feature a through-hole feedline that can attach to directly to the PCB, and they pack the performance (Table 5) of a conventional monopole into an incredibly compact quarter-inch diameter package.

Table 5 ANT-JJB-xx Characteristics [*Antenna Factor Inc.*]

Features	**Electrical Specifications**	
Very low cost	Center Frequency	916 MHz
Ultra compact package	Bandwidth	30 MHz
Easily concealed internally	Wavelength	Quarter wave
Good for internal and external mounting	VSWR	<2.0 typ. at center
Excellent performance	Impedance	50 Ω
Omnidirectional pattern	Connection	Direct Solder

3-1-2-3 ANT- 916-CHP-x

The CHP series antennas [*Antenna Factor Inc.*] utilize Low Temperature Cofired Ceramic (LTCC) technology to embed the antenna element into a ceramic substrate. The high frequency characteristics (Table 6) of this technology enable exceptional performance in a very small package.

Table 6 ANT-916-CHP-x Characteristics [*Antenna Factor Inc.*]

Features	**Electrical Specifications**	
Incredibly compact SMD package	Center Frequency	916 MHz
50 W characteristic impedance	Bandwidth	10 MHz
Low loss	Wavelength	Quarter wave
Wide bandwidth	Pattern	Omni-directional
Favorable linear polarization	Polarization	Linear
>Unity gain	VSWR	< 2.0
No external matching required	Maximum gain	0.5 dBi
Highly stable over temp. and time	Impedance	50 W
Cost effective	Power handling	3 W (max)

3-1-2-4 ANT-315-HETH (or ANT-916-HETH)

The details of this antenna [*Antenna Factor Inc.*] are described in the receiver antenna selection section as these are very directional, and that is very appropriate for our system, which requires a central station feeding multiple modules. The transmitter input was provided by an RF signal generator that generated a peak-to-peak signal of 4.0 V maximum at 315 MHz.

Table 7 lists the RF signal generator characteristics. Due to the power limitation of the RF signal generator, an amplifier stage was inserted to produce 2 watts of power at the transmitter input. Figure 3 depicts the antenna and amplifier test setup. Note that is was out of the scope of this work to develop a dedicated transmitter subsystem, although for the final deployment of the system this will be required.

Table 7 RF Signal Generator Characteristics [*Fluke Mfg. Co.*]

RF Signal Generator	Fluke 6060B	10 kHz–1050 MHz
Amplifier 33 dBm/10 dBm	ZHL-1-2 W	5–500 MHz

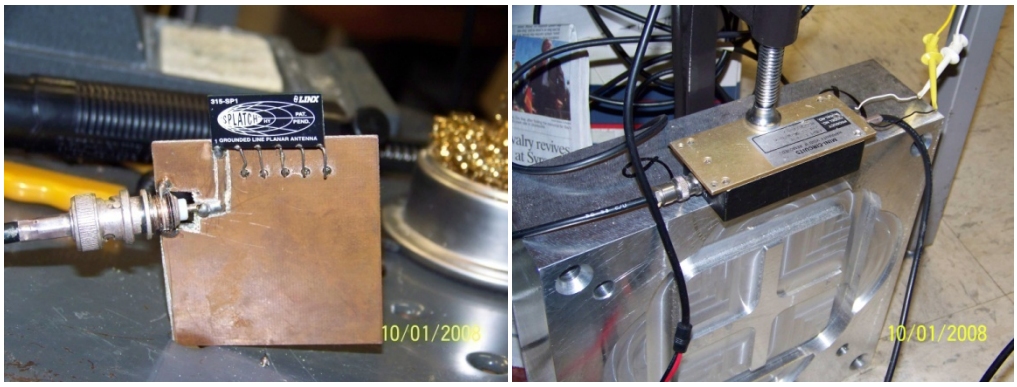

Figure 3 Transmitter fed by the coaxial cable and the amplifier connected to it as the next stage

3-2 Receiver

The transmitted energy has to be captured by a receiver end and this is where we had to decide upon other antennas to satisfy a set of criteria. Receiver antenna characteristics include:

- Directivity. The antenna must be highly directional so that it can receive the power from the transmitter end directly.
- Compact in size. Projected applications have challenging size, weight, and volume constraints.
- Frequency of Operation. The antenna must operate at a frequency suitable to obtain resonance.
- Bandwidth. The antenna shall have a low bandwidth of about 30 MHz.
- Cost. Low recurring cost shall be a requirement for the antenna with a goal of TBD.

3-2-1 Receiver Specifications

The receiver shall be a compact system that will be integrated with the WLSS and shall generate sufficient power to support the worse case operating modes and conditions of the WLSS.

- The receiver system design, including the antenna, matching network, and circuitry, shall meet the weight constraint of TBD. The received power shall meet the minimum requirement for the expected maximum predicted load of the WLSS application. The *frequency of operation* of the receiver circuit compatible with the transmitter frequency of operation.
- Efficient power generation at the receiver requires the *receiver circuit impedance to match* that of the antenna.

The receiver will be integrated with and provide power to the WLSS. DC power shall be generated through rectification of the RF signal received from the remote transmitter. The WLSS including the power system shall be designed to operate during exposure to the induced environmental conditions specified for the WLSS use environment. Additional detailed receiver specifications are listed in Table 8.

Table 8 Receiver Specifications

Weight of the system	100 g	Sensitivity	−99 dBm
Power generated	100 mW	Housing material	TPS material
Frequency	315 MHz	Impedance	50 ohm
I_{max}	50 mA	Cost	TBD
I_{min}	27 mA	V_{max}, V_{min}	3.3 V, 1.8 V

3-2-2 Receiver Antenna Selection

Initially, the same antenna that was evaluated with the transmitter was used for evaluation of the receiver performance. However, these antennas did not provide efficient power transfer. Subsequently, the use of more directional antennas (helical) was investigated and evaluated in order to improve power transfer efficiency.

3-2-2-1 ANT-315-HETH (Manufactured by Antenna Factor)

Compact Helical Antennas

Table 9 lists the critical characteristics of the high directivity helical antenna (Figure 4).

Table 9 Receiver Antenna Characteristics [*Antenna Factor Inc.*]

Center Frequency	315 MHz
Connection	Surface mount
Rugged construction	
Very low cost in volume	

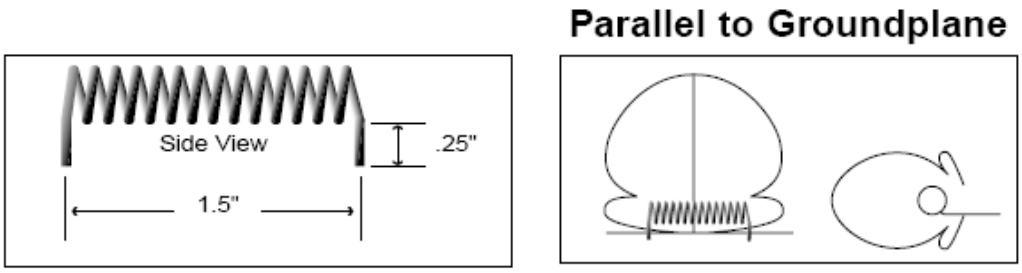

Figure 4 Helical antenna and its radiation characteristics [*Datasheet for ANT-315-HETH, Antenna Factor Inc.*]

3-2-2-2 System Application Concept

It may be appropriate at this point to provide a rough sketch of the system as perceived by us based on the requirements and specifications provided by the customer. Figure 5 shows an overview of the heat shield [*Studor*, 2007; *Jamnejad and Silva*, 2007] and a number of receiver modules present on it for data collection (temperature, pressure, etc.). We envision developing a system whereby power can be fed to these numerous receiver modules from a single transmitting point (shown in the figure, outside the heat shield). Effectively we require an omnidirectional antenna sending power to the directional receiver modules tuned towards the transmitter for efficient power transfer.

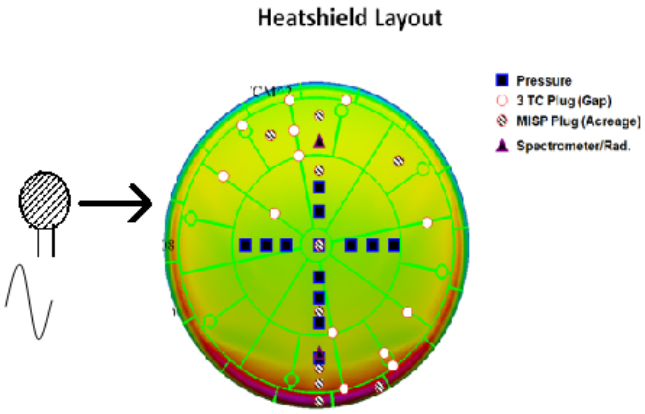

Figure 5 System as envisioned on the heat shield [*Studor*, 2007]

3-2-3 Energy Harvesting Circuit

The RF energy received through the antenna is processed by a multistage rectifier to produce a quasi-DC voltage. More details about the choice of rectifier circuit and the results obtained after the received signal passes through it are given in more detail in the Appendix A.

3-2-4 Antenna Performance Characterization

After fabricating a system model, it was parameterized to analyze its performance. We started first with the data from the Splatch antennas. We built up an apparatus that could orient the antennas with respect to each other and at the same time the distance could be varied. Numerous parameterizations were performed. An example of one such parameterization (Figure 6) is shown below.

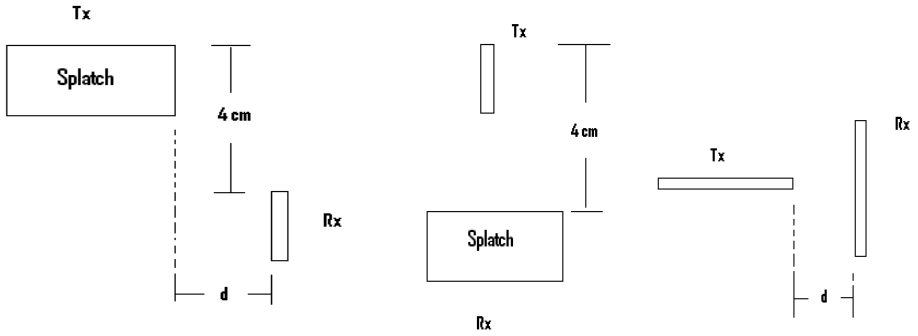

Figure 6 Performance characterization with two Splatch antennas

The setup of Figure 6 shows two Splatch antennas aligned to each other in different configurations and provides the front, side, and top view. The vertical and horizontal distance between the two is about 4 cm. This parameterization was performed at an early stage of the project when the magnetic field coupling in the line of sight of antennas was not explored in great detail. However, once strong fundamentals were established, more directional antennas were used

to demonstrate the proof of concept system, and to show the non-radiative magnetic coupling and power beaming between the transmitter and receiver nodes.

3-3 Energy Storage

Our choice for the energy storage is ultracapacitors [*Dirjish*, 2008] that have an unusually high energy density, typically on the order of thousands of times greater than a high capacity electrolytic capacitor and have smaller size, weight, and volume than batteries.

Charge storage in capacitors is via charge carriers of opposite sign stored on metal places, which creates the potential between the two plates. The energy stored is proportional to the charge stored in this manner and the potential between the plates. Ultracapacitors, on the other hand, have the two plates as the two layers of the same substrate and this results in the effective separation of charge despite the thin physical separation the layers. The lack of a requirement for a bulky layer of dielectric permits the packing of plates with much larger surface area into a given volume, resulting in their extraordinarily high capacitances. Each individual layer is quite conductive, but the interface where the layers are effectively in contact means that no significant current can flow between the layers. However, the double layer can withstand only a low voltage, which means that electric double-layer capacitors rated for higher voltages must be made of matched series connected individual electric double layer capacitors.

In general, these ultracapacitors improve storage density through the use of nanoporous material, typically activated charcoal, in place of the conventional barrier. Activated charcoal is a powder made up of extremely small and very rough particles, which in bulk form a low density volume of particles with holes between them which resembles a sponge. The overall surface area of even a thin layer of such a material is many times greater than a traditional material, allowing many more charge carriers to be stored in any given volume. The downside is that the charcoal takes the place of the improved insulators, so in general electric double layer capacitors use low

potentials on the order of 2 to 3 V. Figure 7 below explains the fabrication of the ultracapacitor and how it is able to provide a high energy density compared to traditional capacitors.

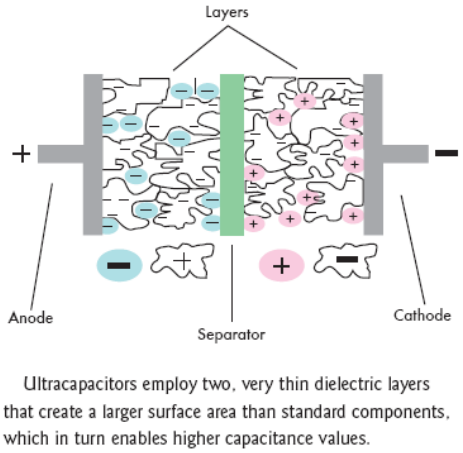

Figure 7 Construction diagram of an ultracapacitor [*Dirjish,* 2008]

We have used the Cap-XX series of ultracapacitors for use in storage of power that is beamed from the transmitter and stored in the receivers. Table 10 lists the specifications [*Dirjish,* 2008] of the ultracapacitor and Figure 8 depicts the ultracapacitor.

Table 10 Specifications of the Ultracapacitor

Power Density	~ 70 kW/liter
ESR	Low
Capacitance	High
Leakage Current	Very low
Voltage rating	4.5 V
Temperature range	−40 to +70 °C
Environmental friendly	
Compact in size	

For tight-quarter portable designs, CAP-XX GS/GW series capacitors sport a slim profile measuring 28.5 by 17 mm and a thickness in the realm of 2.15 to 2.9 mm.

Figure 8 CAP-XX Supercapacitor [*Dirjish,* 2008]

The following plot (Figure 9) is the MATLAB simulation of the ultracapacitor energy storage that was used for power beaming experiments in the lab using helical antennas.

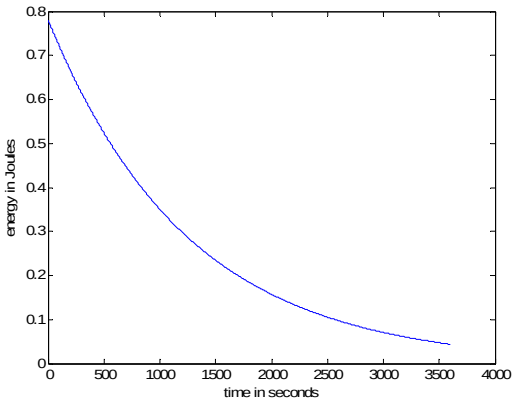

Figure 9 MATLAB simulation of the energy in joules stored in the supercapacitor as a function of time

The use of the energy storage device was selected by comparing components available and research was done to choose the appropriate one taking into account the constraints imposed in terms of weight, energy storage, charge/discharge time, etc. Table 11 shows the comparison of different energy storage devices available and owing to the objective of the project, supercapacitors were employed to be connected to the receiver modules as the choice for powering the communication module and the sensors.

Table 11 Comparison of different Energy Storage Devices

Property	**Cap-XX supercapacitors**	**Capacitors**	**Micro-fuel cells**	**Batteries**
Charge/discharge time	Milliseconds to seconds	Pico to milliseconds	Typically 10 to 300 h	1 to 10 h
Operating temperature	−40 to +85 °C	−20 to +100 °C	+25 to +90 °C	−20 to +65 °C
Operating Voltage	2.3 to 2.75 V/cell	6 to 800 V	0.6 V/cell	1.25 to 4.2 V/cell
Capacitance	100 mF to >2 F	10 pF to 2.2 mF	N/A	N/A
Life	30,000+ hours	>100,000 cycles	1500 to 10,000 h	150 to 1500 cycles
Weight	1 g to 2 g	1 g to 10 kg	20 g to over 5 kg	1g to over 10 kg
Power density	10 to 100 kW/kg	0.25 to 10,000 kW/kg	0.001 to 0.1 kW/kg	0.005 to 0.4 kW/kg
Energy density	1 to 5 Wh/kg	0.01 to 0.05 Wh/kg	300 to 3000 Wh/kg	8 to 600 Wh/kg
Pulse load	Up to 100 A	Up to 1000A	Up to 150 mA/cm^2	Up to 5 A

Chapter 4

Fabrication, Test and Conclusion

This chapter provides a detailed description of the system built in the lab. Some of the results and tests conducted have been tabulated, and after analysis and deliberation, a theoretical explanation of the phenomenon and performance has been stated.

4-1 Proof of Concept System

Numerous tests were performed to confirm the feasibility of the Concept System *viz*. an omnidirectional transmitter module beaming energy to multiple receiver modules (that had to be very directional to capture and store optimum amount of energy. Figure 10 below shows the receiver module that was built and tested on

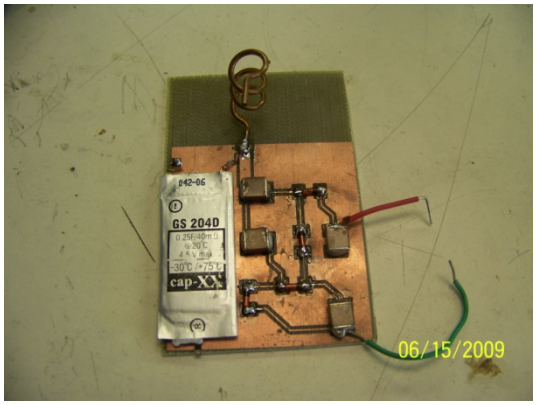

Figure 10 The receiver module built at Penn State consisting of resonant antenna, rectifier circuit, and energy storage ultracapacitor

Most of the requirements on the receiver modules were met in terms of directionality and energy storage using ultracapacitors; however, the efficiency of the system was a major concern. On closer investigation of the coupled-mode theory (which is the model we started with), it can

be seen that the energy transfer between the transmitter (Figure 13) and receiver modules (Figure 14) involves two resonant systems. The energy contained in the coil is due to its inductance, which is treated as a standard oscillator. Inspection of the coupling equation led to the conclusion that the inductive nature of the transmitter and receiver was the prime factor responsible for efficient power transfer. Thus, the inefficiency, or in some cases, the total absence of the power beaming phenomena was most likely due to the use of antennas that had no inductive "coil-kind of body" subsequent to test and evaluation of many antenna, transmitter module, and receiver module configurations and combinations. It was concluded that the helical antenna was the most appropriate to use to transmit and capture energy. Hence, for the results presented here (preliminarily tested on an array of LEDs as shown in Figure 11), we used the ANT-315-HETH instead of the Splatch at the receiver end.

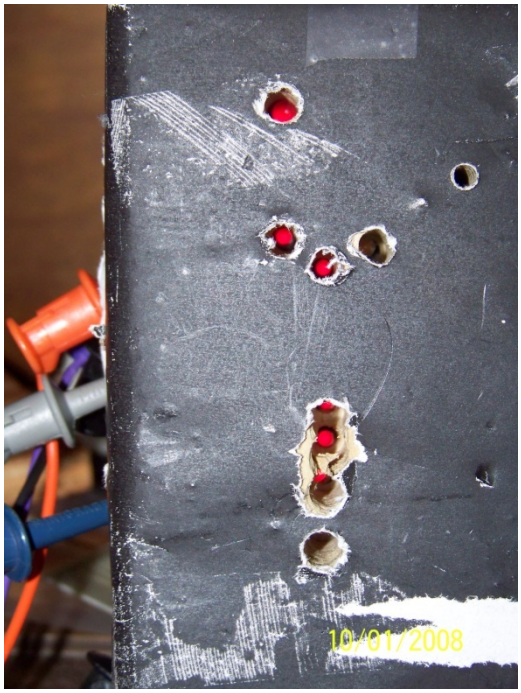

Figure 11 LED array connected to receivers

Figure 12 below shows the plot of SWR of the Splatch antenna when hooked up with a network analyzer. We are still working out the optimization of the helical antennas. However, the

pattern of Splatch is very suggestive about the directivity and operation at the desired frequency range.

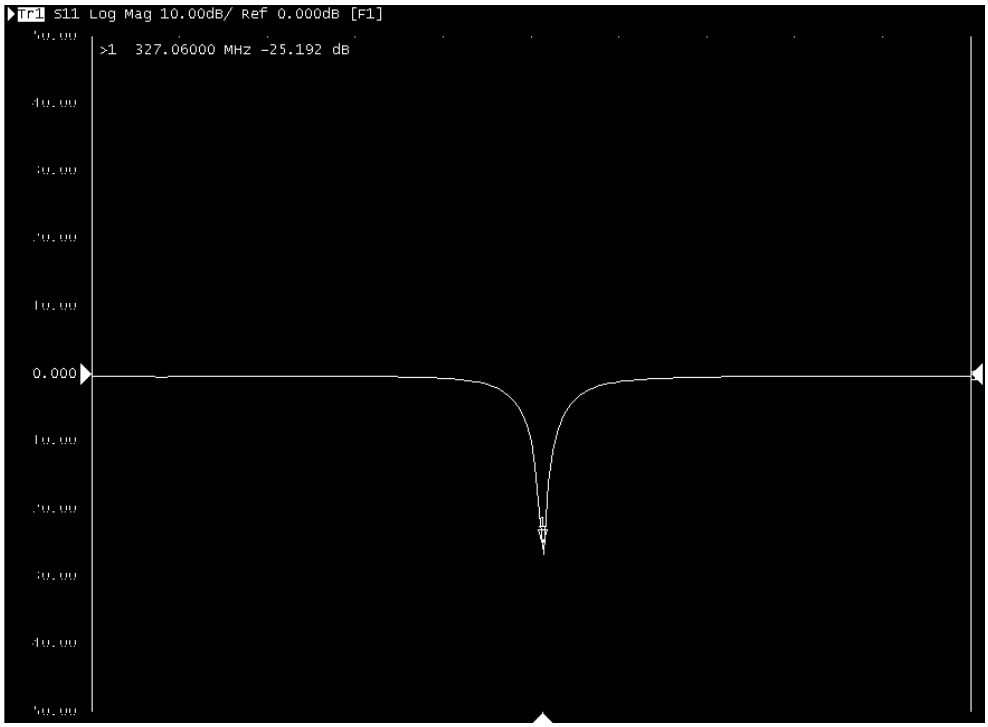

Figure 12 Output from a network analyzer connected to the ANT-315-SP. Note the sharp dip of about 30.0 dB at 327.00 MHz.

4-2 System Testing and Observations

Various tests were performed with the power beaming setup apparatus (Figures 13 and 14) to validate the system and the theoretical assumptions that conceptualized prior to manufacturing the hardware. Some of the more significant and relevant tests are discussed in the following pages.

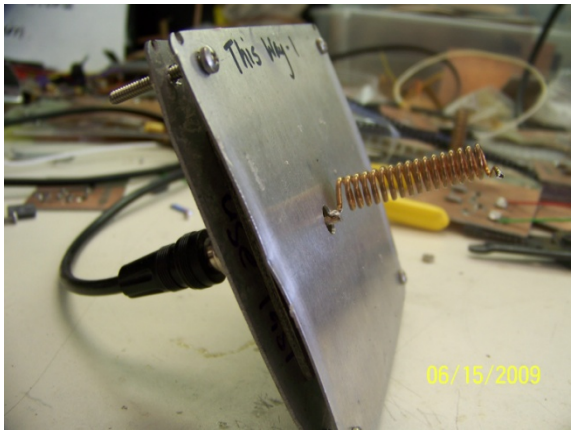

Figure 13 Transmitter end sending signal at 340.00 MHz and the multiple receiver modules that are not receiving any signal since the transmitter is off

Figure 14 LEDs on each of the receiver modules turn on from the power signal that is sent from the transmitter at a distance

The following tables state the power transfer value (Table 12), tests of different orientations of the receiver and transmitter modules (Table 13), and the testing of the modules with the supercapacitors (Table14).

Table 12 Testing with different loads (Jun 7, 2009)

Case	*V* (volts)	*I* (mA)	*P* (mW)
Open Load	17.5		
R = 10 Ω	0.065	4.5	.2925
R = 1 kΩ	2.6	7	18.2
R = 100 kΩ	12.2	7	85.4
R = 1 MΩ	16	6.9	110.4

Table 13 Measuring power transfer using helicals in different orientations on July 15, 2009

Experiment	Voltage (*pk-pk* or max)	Power
Antennas placed about 20 cm away. We use a 10 kΩ resistor	4 V	1.6 mW
With only 2 antennas (315 HETH) placed vertically & distance between them is 20 cms		
10 kΩ	450 mV	25 W
With receiver boards	2.5 V	
Antennas are place horizontally, 20 cm away		
No load	8.6 V	
R=10 Ω	203.1 mV	40 mW
R=1 kΩ (becomes 7 kΩ equivalent)	1.08 V	
R=100 kΩ	8 V	

Table 14 Supercapacitor testing with power beaming, August 11, 2009

Case/Experiment	Voltage across terminals (V)
Brand new supercapacitor	9.6 mV
Supercapacitor hooked to the wireless transmission system:	
50 cm power beaming 20 minutes	0.571
Distance 30 cm, 20 minutes	2.77
Distance 15 cm, 50 minutes	Burnout
Distance 15 cm, 20 minutes	3.3

Following are the tests conducted to improve the efficiency of the system. Components were added (Table 15) to get better matching and higher power transfer efficiency. Table 16 lists the theoretical explanation of components, configurations and the tests that were performed.

Table 15 Testing with the aim of better matching on August 23, 2009

Components used- T_x, R_x boards, supercapacitors, voltage regulators (LM340S), DC–DC convertor (PICO 12SM5D), pots, inductors, and capacitors for matching	
Configuration: T_x and R_x are 10 cm away in all the setups. The output load is an array of 7 parallel LEDs in most cases	Results obtained
Config #1: R_x > DC–DC convertor > Output	
Config #2: R_x >Matching circuit > DC–DC conv > Output	
Config #3: R_x >Supercap > Voltage Regulator > Output	Input off of VR = 2.6 VDC
	NL: V_{in} to VR = 3.47 VDC V_{out} to VR = 2.8 VDC
Config #4: R_x > Voltage regulator > Supercap > Output	Out off of supercap = 1.7 VDC
	Output off of VR = 1.7 VDC (Input to VR = 2.54 VDC)

Table 16 Conclusions of the tests performed as stated above

Config #3	Problem of high voltage output averted
	Issue to address- regulation of input voltage to VR
Config #4	Addressing the issue of choosing the best configuration

Table 17 shows some recent tests conducted and the results tabulated. So far, we have been looking at the power output through the LED output, but here concrete values of power output have been recorded. The discussion of the results is given after, and it describes the error that was being made all the way through to compute the power efficiency, and how it was rectified in the later stages of research.

Table 17 Efficiency calculations

Experiments performed with the objective of measuring power efficiency (Oct. 2009)				
		$V_{p\text{-}p}$	$V_{\max}$	$V_{\min}$
Test #1	Open load voltage off of amplifier	42.34 V	21.41 V	20.94 V
	With 1-kΩ load	15.31 V	7.656 V	7.656 V
	R_x @ 20cm away, Open	7.1 V	518 mV	
	R_x @ 20 cm away, 1-kΩ load	362 mV	7.1 V	
Test #2	Voltage off of amplifier across 82 Ω	13 V	7.1 V	
	Power consumed by the LED	20 mW to 30 mW		
	Efficiency @ 20 cm away	**~9%**		

Test #1 clearly illustrates that the results are far from satisfactory, but the basic error committed in computing the power efficiency is the reason for the same, and it was rectified as recorded in Test #2.

The very poor efficiency was very suggestive, and there had to be a reason for this low value. On close examination, it was understood that owing to the impedance values that were taken as 1 kΩ for the power calculations were incorrect. The amplifier output is dependent on the load impedance connected at its output. Hence, the impedance of the transmitter was calculated using a network analyzer, which is a strong function of the frequency. For the particular frequency at which the power beaming was observed, the impedance value was recorded, and the calculations were performed using this value. Furthermore, the power output at the receiver side was calculated using the specification sheet of the LED, as the output resistance was very difficult to compute due to the presence of a large number of diodes and capacitors in the receiver circuit. This resulted in giving a comprehensive analysis of the amount of power transmitted and received at both the ends separated by a certain amount of distance.

4-2-1 Formulation of Theory from Results and Observations

Results from the numerous experiments with the system led to the hypothetical theory about the power beaming phenomenon, and this section explains the conceptual formulation of the system.

There is energy contained (stored) in the coil, according to its capacitance and inductance value:

$$U = \frac{1}{2} L |I_0|^2 = \frac{1}{2C} |q_0|^2 . \tag{6}$$

The coil is treated as a standard oscillator as explained by the coupled mode theory,

$$\dot{a}_m(t) = (j\omega_m - \Gamma_m) a_m(t) + \sum_{n \neq m} j\kappa_{mn} a_n(t) + F_m(t),$$

where $|a(t)|^2 = \frac{L}{2} |I_0|^2$ is the energy stored in the coil. The ohmic and radiation resistance result in defining the decay constant, Γ. We can also find the coupling coefficient, $\kappa_{Tx,Rx}$ which follows the relation $\kappa \propto D^{-1/3}$. Also, κ and Γ are functions of frequency, and efficiency is maximized for a particular value of *f*. This, we think, might be the reason why the omnidirectional, "non-coiled" antennas are unable to provide power beaming as there is no power stored (due to the non existence of *L* and *C*). We also deal with mutual inductance, which might be an issue for the non-coiled objects, and

$$\kappa = \omega M / \left[2 (L_T L_R)^{1/2} \right]. \tag{7}$$

This implies that if the distance is increased or reduced, then the resonant frequency would also change correspondingly. This means that we need to fix the value of the distance and determine the frequency of resonance at that distance, and this is the frequency at which the majority of the energy needs to be beamed.

Note that the resonant frequency of the antenna is not the frequency of the system. This frequency of operation depends on other factors like: (a) receiver circuit, (b) decay rate Γ, (c) coupling coefficient κ, etc. Tests conducted using various kinds of antennas suggested that the antenna frequency is not the resonant frequency. Specifically, the helical antennas resonating at around 346.00 MHz were the most appropriate to explain most of the formulated theories.

So, at this point, we can specify the ideal power beaming apparatus that can be placed on the heat shield for the power beaming system. The main factor for achieving high efficiency is when $\kappa^2/\Gamma_T\Gamma_R > 1$, and the efficiency is improved by $\omega^2/\Gamma_R{}^2$ (about 10^6) relative to the case of only inductively coupled non resonant objects. Since $\kappa \propto 1/\sqrt{L_T L_R}$, this implies that if the inductance L is large, then the coupling between the receiver and the transmitter system is reduced. But the decay constant, $\Gamma \propto 1/L$, works in the counter fashion in that if the inductance is large, the decay is lower. Hence, the underlining results of all this analysis are that κ and Γ balance out each other at a certain frequency as discussed previously. The above are some results and analysis that helped us formulate our theory, and it is open for discussion. But our results corroborate the theory to a satisfactory extent.

4-3 Miscellaneous Considerations

We end here with

- We have to take into account (Table 18) the *average distance between the power source (transmitter) and the sensor module*, which is to be carefully decided as we want to obtain maximum efficiency from the transmitter/receiver system
- Control/adjust the *maximum distance* between the node and power transmitter to obtain appreciable power to keep the sensor modules in operation.

- System operating life is an important characteristic to assure mission success in hostile use environments. We approximate the number taking into account the temperature and pressure conditions

Table 18 Miscellaneous Components Specifications

Average distance between module and power source	2 m
Maximum distance	5 m
Minimum distance	0.3 m
System life	>10 years
Total cost	TBD

Chapter 5

Summary and Future Work

The overall theme of this work is to develop a system whereby power can be transferred without any physical linkage between the receiver and transmitter sides. A particular application domain is emphasized that deals with the powering of sensor modules on a spacecraft during re-entry into the planetary atmosphere. With the current arrangement of cables running all over these spacecraft, and the problems associated with cutting the cables when the heat shield detaches and so on, this system provides a means to tackle these issues.

The basic working of the phenomenon has been established and conceptualized. The use of near field, nonradiative coupling of magnetic fields at a resonant frequency is tested and observed and various aspects of the procedures are tabulated to illustrate the ingenuity of the research. Understandably, most of the work is in an early stage owing to the timeframe, but it clearly establishes concept credibility and viability for further improvements and validation of the theory and the conceptualized baseline system.

Some of the basic issues concerning efficiency of the power transfer and detecting the resonant frequency mathematically are areas for additional research. But it has clearly been established that the technology is very much operational, and Table 19 suggests some ways that the current system can be updated to move into the next phase of the project.

5-1 Improvements on the Existing System

Improved antennas are required to improve performance of the baseline system (Table 19). The antennas currently used do not have good resonance characteristics, they essentially are

helical monopoles, and do not have a particularly good response. Getting a compact (preferably helical) antenna would result in have a more efficient power beaming system.

The testing of the system was done on a marginally rigid mechanical system. More repeatable, reliable results would be obtained with a more robust design of the mechanical assembly.

The current modules have been designed using off-the-shelf readily available components, which were used owing to their functionality, and not optimization. Thus, a better designed system would be the result of a properly and well researched list of components with a thorough understanding the operation of the analog circuit functionality. The use of a feedback loop for two purposes would be very helpful; one for tuning the receiver and transmitter modules in terms of frequency (it has been discussed above about the sensitivity of the resonance with distance), and secondly for controlling the power output at the receiver end. This has a lot to do with the energy storage device utilized.

This also brings up the implications of the power storage component, and more elaborate analysis of the components available, keeping in mind the ratings (which is an important criterion for the application) of the same.

Lastly, it would be very interesting to test the system for higher power applications. So far, the sensor modules act as the receivers and they consume a few milliwatts of power, for which a few hundred milliwatts of power are transmitted right now. As was referenced in one of the research papers [*Karalis et al.,* 2008], in which high power applications were tested that yielded an efficiency of about 40%, it is very suggestive to test out the system with high power components.

Table 19 Future scope of the system

Suggestions	Comments
Better Antennas	Directionality ensures better coupling (although some analysis shows that it may not be entirely true)
More mechanically rigid test setup	For better testing
Better assembled PCBs at the receiver end	More research into rectifier circuits might yield some better results (More research into the components used)
Use of tunable circuits (automatic feedback loops)	More scope of tuning would ensure the best efficiency
Feedback loop to attain the point of maximum resonance	It was observed that the frequency changes with distance
Testing for higher power	So far, only low power applications have been tested. It will be very interesting to work on high powered applications
Look into better energy storage devices	So far, the supercapacitors used are less than optimal
Possibly have a feedback loop for the energy storage	This will result in better control of power output

Appendix A

ZigBee Modules

For this project we chose ZigBee modules (Figure 15) to be the wireless protocol used to transmit data between sensor nodes and the data acquisition node. The choice has been made based on its low power consumption and other parameters as stated in Table 20.

Figure 15 One of our modules [*Studor*, 2007]

Table 20 Zigbee Module Specifications

Parameter	Value
Data rate	250 kbits/sec
Range	10–100 m
Networking topology	Ad-hoc, peer to peer, star or mesh
Operating frequency	2.4 GHz
Power consumption	Very low
Operating ambient temperature range	−40 to +85 °C
Operating supply voltage	2.0–3.6 V

Appendix B

Rectifier circuit details

Described here is the double stage rectifier that was used at the receiver side to convert the RF sinusoid into DC voltage to provide to the load. The circuit consists of a bank of capacitors and diodes that rectify the incoming sinusoidal signal. The larger the number of rectifier stages, the smoother the rectified waveform. The rectification occurs as a result of storage of energy in the capacitors and due to the diode's property that allows only positive values of signal to pass through it (ideally). Full rectification results in rectifying both the positive and the negative cycles of the signal. As can be seen in Figure 16 the sinusoid (green) is rectified (blue) when passed through a double stage rectifier (Figure 17).

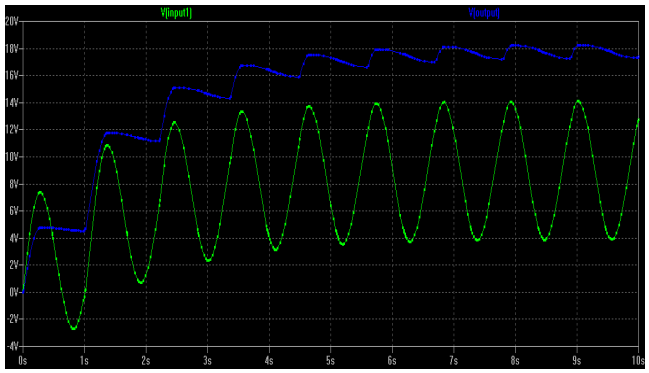

Figure 16 SPICE simulation of the rectifying circuit

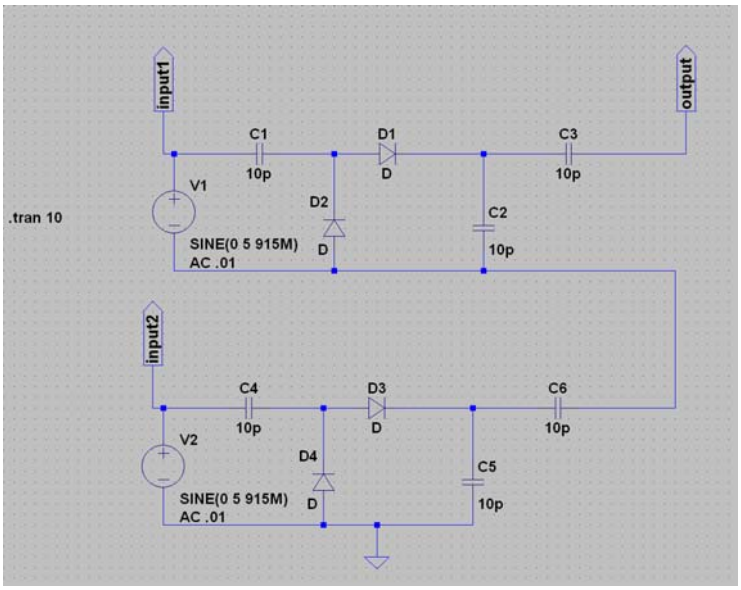

Figure 17 Circuit of the two stage rectifier

Appendix C

Parameterization Example

The details of the data obtained with the configuration (stated before in the thesis) are given in this section (Table 21).

Table 21 Parameterization data using Splatch antenna

D (in cm)	V_{max} (mV)	V_{pp} (mV)	V_{min} (mV)
0	320	225	95
1	156.3	198.4	−42.1
2	101.6	171.9	−70.3
3	75	143.8	−68.75
5	45	98.75	−53.75
7	49.4	105	−55
10	40.6	80	−39.4
15	26.9	60	−33.1
20	24.4	55.6	−31.25
25	29.4	58.7	−29.4

The DC output (Figure 18) is connected to a series/parallel array of LEDs that light up when the power is beamed through the air.

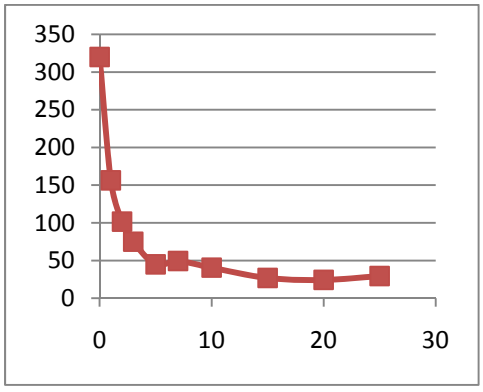

Figure 18 Graph of the parameterization data output

Appendix D

Sensors for the Communication Modules

Sensors are another component that drive the power requirements of our system because a certain fixed amount of power at a certain temperature is needed to collect data. The data is then processed using the ZigBee modules (to which these sensors are connected) and transmitted.

Hollow Aerothermal Ablation Temperature (heat) Sensor (*Courtesy of NASA Ames Research Center*)

The Ames HEAT Sensor is a sensor designed to track the progression of a ~700 °C isotherm layer through an ablative thermal protection system material. A sensor is constructed (Table 22) by wrapping resistive platinum-tungsten wire around a polyimide tube and sheathed with a liquid polyimide coating (Figure 19). After construction, the sensor (Figure 20) is embedded in a hole drilled through the TPS material.

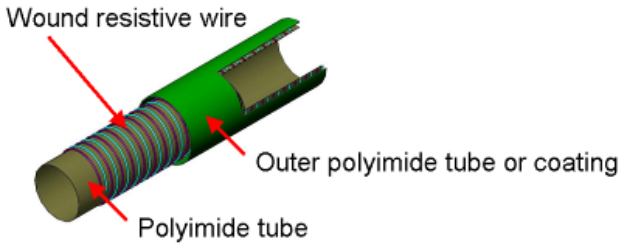

Figure 19 Schematic of a HEAT sensor

When excited with a constant current source, the sensor's resistance will decrease following the isotherm progression through the surrounding TPS material. This resistance measurement is then converted to a length measurement through the sensor's resistance/length coefficient.

Table 22 Heat Sensor Characteristics

Sensor length-matched to TPS material, Sensor diameter	0.2 cm
Sensor mass	1.7 g
Resistance/Length conversion factor	69.75 Ω/mm
Current source (excitation)	Variable, but 0.5–1 mA provided by external electronics is typical

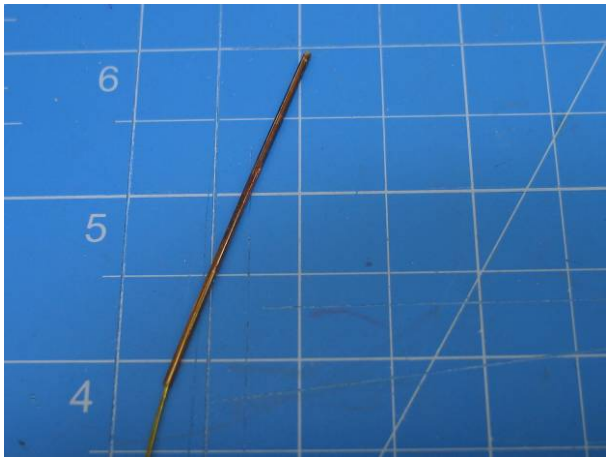

Figure 20 Photograph of a HEAT sensor

ISP Thermal Sensor (*Ames Research Center*)

The Ames ISP Thermal Sensor (Figure 21) is a sensor designed to make temperature and heat flux measurements for thermal protection system instrumentation applications. It is composed of platinum ink resistance temperature detectors (RTDs) screen-printed on both sides of an alumina ceramic disk. The thermal sensor is capable of measuring up to 1500 K and ~30 W/cm^2 of heat flux.

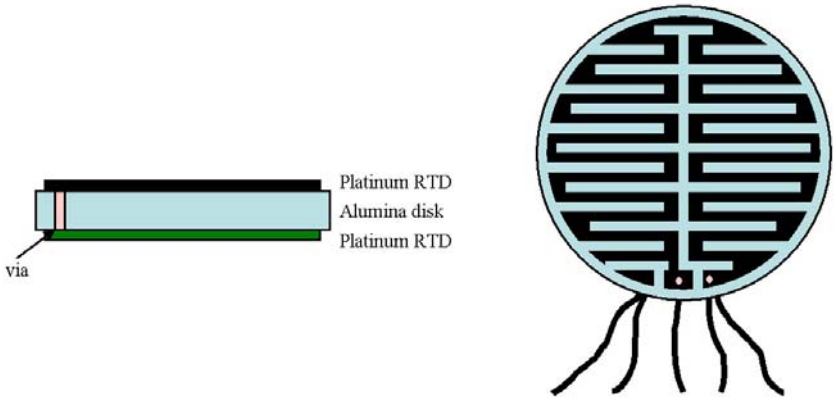

Figure 21 Schematic of Ames ISP Thermal sensor showing side and top-down view

The thermal sensor (Figures 22 and 23) operates by measuring (Table 23) the resistance of the two sensor faces and reducing the data to determine temperature and heat flux. Depending on the application, both RTD's are measured separately or in series. An external current source is required to provide excitation to the sensor. Platinum wires with Kapton sheaths are welded onto the sensor pads.

Table 23 Thermal Sensor Characteristics

Size		**Wire assignments (4-wire RTD)**	
Sensor thickness	500 μm	Wire 1	Sense top (+)
Sensor diameter	1 cm	Wire 2	Sense top (−) & Sense bottom (+)
Sensor mass	1 g	Wire 3	Sense bottom (−)
Sensor line width	100 μm is typical	Wire 4	Excitation (+)
		Wire 5	Excitation (−)
Current source (Excitation)			
Variable but 0.5 mA provided by external electronics is typical			
Temperature to resistance conversion with 0.5 mA excitation			
25 °C		200 Ω	
600 °C		650 Ω	
1000 °C		1000 Ω	
Power consumption			
25 °C		0.1 mW	
600 °C		0.325 mW	
1000 °C		0.5 mW	

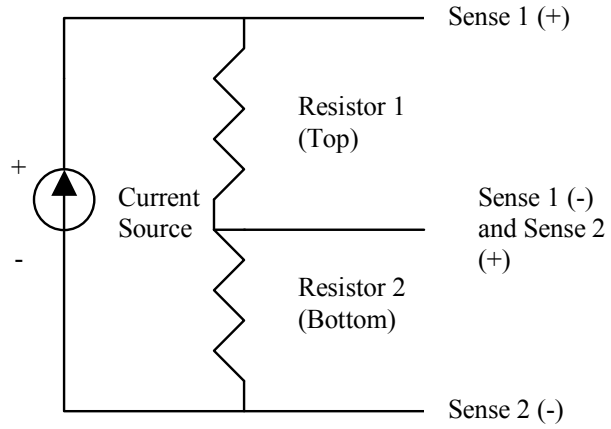

Figure 22 Electronic-equivalent schematic of thermal sensor

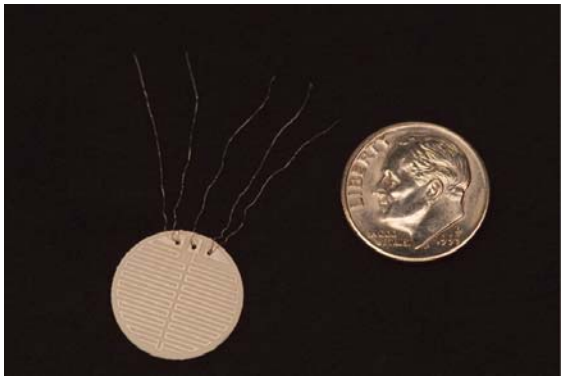

Figure 23 Photograph comparing thermal sensor size with that of a dime

Appendix E

Development of an Arc jet Test Regimen

Much of the work in the Summer and Fall of 2009 has focused on designing an experiment and system that can be tested in the arc jet facility at NASA Ames in the late 2009–early 2010 timeframe. This experiment will serve two primary purposes. First, it will indicate whether or not it is feasible to replace wiring bundles for sensors (Figure 24) in test environments such as that of the arc jet facility [*NASA Ames Research Center*] (Figure 25). Second, it will serve as a test of the modules under development in a relevant (albeit harsher) environment and provide guidance for continued development of the modules.

Figure 24 Wiring bundles

Figure 25 Harsh environment of the Arc Jet facility

The wireless sensor node prototypes will be validated in harsh environments by including it in a test of a Thermal Projection System material. The test will occur at NASA Ames Research Aerodynamic Heating Facility (AHF) with heating parameters equivalent to a 10-kg small probe re-entry at a specific flight path that will be formulated using COBRA.

In this test, the wireless sensor node will be embedded in the insulation layer. This placement of the sensor module will provide the greatest amount of thermal protection for the system. The node will be attached to four embedded thermocouples, which will be sampled at 10 Hz with 14-bit resolution. The system will then relay the information to the ZigBee baseline station outside of the test chamber where it will be integrated into a National Instruments LabVIEW-based interface. The thermocouples will also be attached to the currently used wired data acquisition system to allow for comparison of data and give a baseline data package for validation of the wireless system.

Previous tests to validate designs from previous work occurred only in the NASA Ames X-Jet Facility. The change from the X-Jet to the AHF is a significant step due to the increased temperatures and electromagnetic interference experienced during the test in comparison to the X-Jet. The outcome of this test (scheduled to be performed in early 2010) will hopefully both

validate the overall concept of a wireless sensor network in harsh environments as well as give credence to continued work on wireless sensors for future unmanned and manned missions.

References

Antenna Factor, *Datasheets*, ANT-315-SP, ANT-315-HETH, ANT-916-JJB-xx, and ANT-916-CHP-x.

Brodowsky, W. Heitmann, and G. Nimtz, "Comparison of experimental microwave tunneling data with calculations based on Maxwell's Equations," *Physics Letters* A 222, pp. 125–129, 1996.

Brown, William, "The History of Power Transmission by Radio Waves," *IEEE Transactions on Microwave Theory and Techniques,* Vol. MIT-32, No. 9, pp. 1230–1242, 1984.

Carniglia, C.K and, L. Mandel, "Quantization of Evanescent Electromagnetic Waves," *Phys. Rev. D,* Vol. 3, No. 2, pp. 280–296, 1971.

Cossio, Carlos, "Wireless battery energizes low power devices," *Design Ideas*, pp. 79–80, Nov. 2007.

Deych, Lev I., D. Livdan, and A. A. Lisyansky, "Resonant tunneling of electromagnetic waves through polariton gaps," *Phys. Rev E*, Vol. 57, No. 6, pp. 7254–7258, 1998.

Dirjish, Mat, "Ultracapacitors branch out into wider markets," *ED Online* ID#20034, Nov. 2008.

Enders, A., and G. Nimtz, "Evanescent-mode propagation and quantum tunneling," *Phys. Rev E*, Vol. 48, No. 1, pp. 632–634, 1993.

Imura, Takehiro, Hiroyuki Okabe, and Yoichi Hori, "Basic Experimental Study on Helical Antennas of Wireless Power Transfer for Electric Vehicles by using Magnetic Resonant Couplings," *Vehicle Power and Propulsion Conference,* 2009.

Jamnejad, Vahraz, and Arnold Silva, "Microwave Power Beaming Strategies for Fractioned Spacecraft Systems," *IEEEAC* Paper No. 1549, Ver. 3, Nov. 2007.

Jiang, Jehn Ruey, Yung-Liang Lai, and Fu-Cheng Deng, "Mobile Robot Coordination and Navigation with Directional Antennas in Positionless Wireless Sensor Networks," *Proceedings of the International Conference on Mobile Technology, Applications and Systems*, Article no. 80, 2008.

Karalis, Ariseidis, J.D. Joannopoulos, and Marin Soljacic, "Efficient wireless non-radiative mid-range energy transfer," *Annals of Physics*, Vol. 323, pp. 34–48, 2008.

Krishnan, “Method and Apparatus for Wireless Powering and Recharging,” *United States Patent* No. 6,127,799, 2000.

Kurs, Andre, Aristeidis Karalis, Robert Moffatt, J.D Joannopulos, Peter Fischer, and Marin Soljacic, “Wireless Power Transfer via Strongly Coupled Magnetic Resonances,” *Science*, Vol. 317, pp. 83–86, 2007.

Mecke, C. Rathge, “High Frequency Resonant Inverter for Contactless Energy Transmission over Large Air Gap,” *IEEE Annual Power Electronics Specialists Conference*, 2004.

Mi, Minhong, Marlin H. Mickle, Chris Capelli, and Harold Swift, “RF Energy Harvesting with Multiple Antennas in Same Space,” *IEEE Antennas and Propagation Magazine*, Vol. 47, No. 5, pp. 100–106, 2005.

Mickle *et al*., “Apparatus for energizing a remote station and related method,” *United States Patent* No. 6,615,074 B2, 2003.

Popovic, Zoya B. “Wireless Powering for Low-Power Distributed Sensors,” *Serbian Journal of Electrical Engineering*, Vol. 3, No. 2, pp. 149–162, 2006.

Salter, Thomas, George Metz, and Neil Goldsman, “Improved RF Power Harvesting Circuit Design,” *Semiconductor Device Research Symposium*, December 12–14, 2007.

Scheible *et al.*, “System for wirelessly supplying a large number of actuators of a machine with electrical power,” *Patent Pub*. No. US2002/0118004 A1, 2002.

Studor, George, “Fly-by-Wireless: A Revolution in Aerospace Architectures for Instrumentation and Control,” *NASA CANEUS Workshop*, 2007.